CALCULATED DIPOLE MOMENT
AND ENERGY IN COLLISION
OF A HYDROGEN MOLECULE
AND A HYDROGEN ATOM

by R. W. Patch

Lewis Research Center

Cleveland, Ohio 44135

1. Report No. NASA TM X-2839	2. Government Accession No.	3. Recipient's Catalog No.
4. Title and Subtitle CALCULATED DIPOLE MOMENT AND ENERGY IN COLLISION OF A HYDROGEN MOLECULE AND A HYDROGEN ATOM		5. Report Date July 1973
		6. Performing Organization Code
7. Author(s) R. W. Patch		8. Performing Organization Report No. E-7342
9. Performing Organization Name and Address Lewis Research Center National Aeronautics and Space Administration Cleveland, Ohio 44135		10. Work Unit No. 503-04
		11. Contract or Grant No.
12. Sponsoring Agency Name and Address National Aeronautics and Space Administration Washington, D. C. 20546		13. Type of Report and Period Covered Technical Memorandum
		14. Sponsoring Agency Code

15. Supplementary Notes

16. Abstract

Calculations were carried out using three Slater-type 1s orbitals in the orthogonalized valence-bond theory of McWeeny. Each orbital exponent was optimized. The H_2 internuclear distance was varied from 7.416×10^{-11} to 7.673×10^{-11} m (1.401 to 1.450 bohrs). The intermolecular distance was varied from 1 to 4 bohrs (0.5292 to 2.117×10^{-10} m). Linear, scalene, and isosceles configurations were used. A weighted average of the interaction energies was taken for each intermolecular distance. Although energies are tabulated, the principal purpose was to calculate the electric dipole moment and its derivative with respect to H_2 internuclear distance.

17. Key Words (Suggested by Author(s)) Dipole moment Hydrogen Intermolecular energy	18. Distribution Statement Unclassified - unlimited

19. Security Classif. (of this report) Unclassified	20. Security Classif. (of this page) Unclassified	21. No. of Pages 38	22. Price* $3.00

CONTENTS

CALCULATED DIPOLE MOMENT AND ENERGY IN COLLISION OF A

HYDROGEN MOLECULE AND A HYDROGEN ATOM

by R. W. Patch

Lewis Research Center

SUMMARY

Ab initio calculations of the interaction energy and electric dipole moment of a hydrogen molecule (H_2) colliding with a hydrogen atom (H) were carried out on a digital computer using three Slater-type 1s orbitals in the orthogonalized valence-bond theory of McWeeny. Each orbital exponent was optimized. The internuclear distance in the H_2 molecule was varied from 7.41599×10^{-11} to 7.67292×10^{-11} meter (1.401446 to 1.450000 bohrs). The intermolecular distance was varied from 0.529167×10^{-10} to 2.11667×10^{-10} meter (1 to 4 bohrs). Linear, scalene, and isosceles configurations were used. A weighted average of the interaction energies of the three equilibrium configurations was then taken for each intermolecular distance.

The interaction energies obtained appear to be qualitatively correct but are higher than a number of published curves. This is because of the simple model used. The electric dipole moment should not be so sensitive to the model.

The electric dipole moment and its derivative with respect to H_2 internuclear distance were consistent with classical values at large intermolecular distances with one minor exception, which is explained. Both sets of values are intended for use in calculating pressure-induced vibrational absorption coefficients in the infrared.

INTRODUCTION

In high-temperature propulsion devices such as gas-core nuclear rockets, an important mechanism of heat transfer is radiant energy exchange between volumes of gas and between the gas and the wall. When such devices use high-pressure hydrogen, it is necessary to know the strength of pressure-induced infrared absorption to calculate the heat transfer. This strength depends on the interaction energy and electric dipole moment of the two colliding chemical species. The strength has been calculated for two

colliding hydrogen molecules (H_2) (ref. 1) but not for H_2 colliding with a hydrogen atom (H). For this second case, which is the motivation of this report, the interaction energy is fairly well agreed upon (ref. 2), but the electric dipole moment had never been calculated. For large intermolecular distances the electric dipole moment can be found from the quadrupole moment of H_2 and the polarizability of H, but for small intermolecular distances the H_3 wave function must be known.

The object of the work described herein was to calculate the electric dipole moment and its derivative and energy after determining the H_3 wave function. The energy was desired only for comparison with experiments and other calculations.

Past work on H_2-H interaction may be divided into ab initio calculations, semiempirical calculations, and experiments. These three types of work will be discussed in subsequent paragraphs.

Ab initio calculations for H_2-H or H_3 have been carried out by a large number of investigators (refs. 3 to 31). Much of the early work utilized rough approximations for some of the molecular integrals, making it of little contemporary value. This pitfall was avoided by Hirschfelder, Eyring, and Rosen (ref. 3), Hirschfelder, Diamond, and Eyring (ref. 4), and Hirschfelder (ref. 6), who exhausted a basis of three 1s atomic orbitals centered on the protons. More recently, Shavitt, Stevens, Minn, and Karplus (ref. 27) exhausted a basis of 15 orbitals (1s, 1s', $2p_x$, $2p_y$, $2p_z$ on each proton). This work was extended by Porter, Stevens, and Karplus (ref. 30). The most accurate work, however, is probably that of Conroy and Bruner (ref. 26), who improved the electron correlation by using a wave function that was the product of a shape series, a singlet-pair correlation series, and a triplet-pair correlation series.

A large number of semiempirical calculations for H_2-H or H_3 have also been made. For large intermolecular distances the treatments of Margenau (ref. 32) and Mason and Hirschfelder (ref. 33) are noteworthy. For small intermolecular distances, the treatment of Porter and Karplus (ref. 2) correlates experimental data best. None of these are useful in finding electric dipole moment.

Experimental studies of H_2-H interaction are also numerous. Amdur (ref. 34) measured the scattering of an H-atom beam in H_2 gas. The potential he obtained is lower than that of Porter and Karplus (ref. 2). Schulz and LeRoy (ref. 35) measured the rate for the reaction

$$H + p-H_2 \rightarrow o-H_2 + H$$
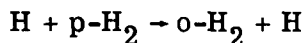
in a flowing system. Karplus and Porter (ref. 36) compared this with the potential of Porter and Karplus (ref. 2) and found fair agreement. Geddes, Krause, and Fite (ref. 37) used modulated crossed beams to obtain the reaction

$$D + H_2 \rightarrow HD + H$$
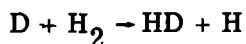
They measured velocities and angular distribution of HD. Brumer and Karplus (ref. 38) found that the results of reference 37 agreed with the potential of Porter and Karplus (ref. 2).

In this study no attempt was made to do the most sophisticated possible ab initio calculation for H_2 - H because accuracy within a few percent for the dipole moment was all that was desired. To achieve this, a full valence-bond ab initio calculation for H_2 - H was carried out with accurate values for all molecular integrals. In order to cover nuclear configuration space, linear, scalene, and isosceles configurations (see fig. 1) were included with intermolecular distances from 0.529167×10^{-10} to 2.11667×10^{-10} meter (1 to 4 bohrs). In three of the configurations (figs. 1(a), (c),

(a) Linear configuration A with equilibrium internuclear distance.

(b) Linear configuration B with greater-than-equilibrium internuclear distance.

(c) Scalene configuration C with equilibrium internuclear distance.

(d) Scalene configuration D with greater-than-equilibrium internuclear distance.

(e) Isosceles configuration E with equilibrium internuclear distance.

(f) Isosceles configuration F with greater-than-equilibrium internuclear distance.
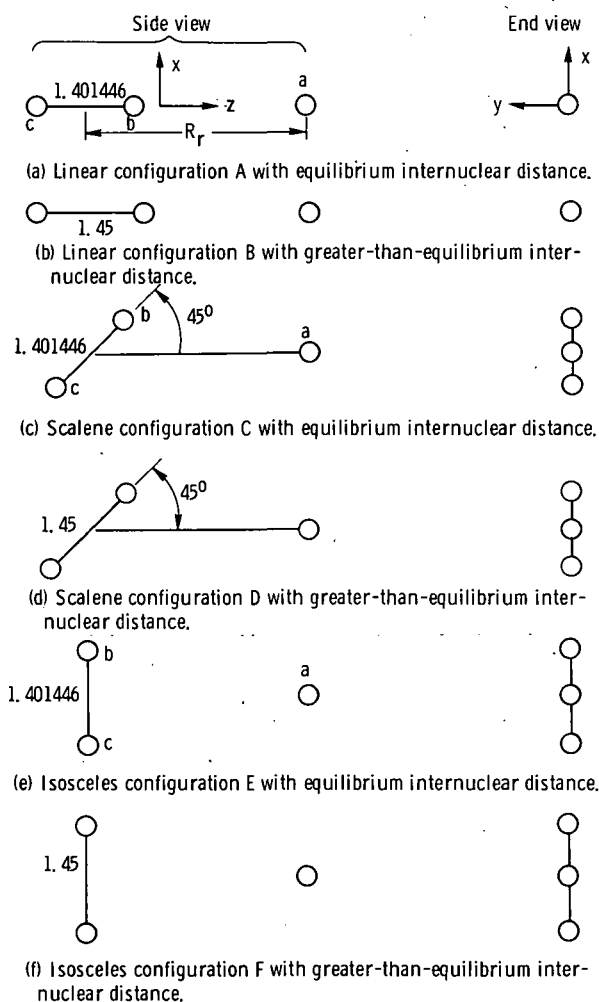
Figure 1. - Six configurations of a hydrogen molecule and a hydrogen atom used in calculations. Intermolecular distance R_r had values from 0.53×10^{-10} to 2.12×10^{-10} m (1 to 4 bohr). Internuclear distances in the figure are in bohrs (1 bohr = 5.29167×10^{-11} m).

and (e)) the H_2 molecule had equilibrium internuclear distance. The average H_2 - H interaction energy was then calculated for a given intermolecular distance by taking weighted averages of the interaction energies of these three configurations. In the other three configurations (figs. 1(b), (d), and (f)) the H_2 molecule had a greater-than-equilibrium internuclear distance so that the derivative of the dipole moment with respect to internuclear distance could be calculated from the electric dipole moment of all six configurations.

Professor V. Magnasco of the Istituto di Chimica Industriale dell'Universita, Genoa, provided listings and a deck of various computer programs for evaluating molecular integrals. Although these programs were not used for this report, they were useful for checking and provided ideas for the programs that were used.

ANALYSIS

Model and Configurations

The interaction of H_2 and H may be calculated by the orthogonalized valence-bond theory of McWeeny (refs. 39 and 40), which utilizes symmetrically orthogonalized atomic orbitals in the Born-Oppenheimer approximation. In this method orthogonalized orbitals are formed from linear combinations of atomic orbitals. These are multiplied by spin eigenfunctions to give orthogonalized spin orbitals. Formal orthogonalized valence-bond structures are formed from linear combinations of antisymmetrized products of the orthogonalized spin orbitals. The system wave function consists of linear combinations of these structures. This involved procedure merely amounts to taking the proper linear combination of the hextuple products of three atomic orbitals and three spin eigenfunctions. This method allows full configuration interaction without unduly complicating a digital computer program and allows straightforward calculation of the electric dipole moment. It has previously been successfully applied to the interaction of two H_2 molecules by Magnasco and Musso (refs. 41 and 42) and Patch (ref. 43).

The model chosen had a basis of three 1s Slater-type atomic orbitals χ_p centered on the protons and had full configuration interaction. The three normalized 1s atomic orbitals were

$$\chi_p(i) = \left(\frac{\zeta_p^3}{\pi}\right)^{1/2} e^{-\zeta_p r_{pi}} \quad p = a, b, c \tag{1}$$

where the i in parentheses indicates the ith electron, and r_{pi} is the distance between proton p and electron i (symbols are given in the appendix). An orbital $\chi_p(i)$, of course, reduces to the wave function for the ground state of an H atom if $\zeta_p = 1.88976 \times 10^{10}$ reciprocal meters (1.0 bohr^{-1}).

If all the atomic orbitals were assigned the same orbital exponent ζ, the model would not accurately represent H_2 + H at large intermolecular distances because isolated H_2 and H have different optimum orbital exponents. If the two orbital exponents belonging to orbitals centered on H_2 protons were assigned the value for isolated H_2, and the other was assigned the value for isolated H, inconsistencies at small intermolecular distances would result (the linear symmetric configuration would have different orbital exponents for the end protons, and the equilateral triangle configuration would have unequal orbital exponents). Hence, each orbital exponent was optimized for each intermolecular distance and each H_2 internuclear distance of each configuration.

In ab initio calculations the average interaction energy should be based on the energy of the complex minus the energies of the two separated chemical species (in this case H_2 and H) calculated in a consistent manner. In the limit of infinite intermolecular distance, the model in this report results in an H atom and a molecule (H_2) described by the covalent-ionic valence-bond model of Weinbaum (ref. 44). Because of the ultimate application of this report to pressure-induced absorption, the experimental equilibrium internuclear distance of 7.41599×10^{-11} meter (1.401446 bohrs) for H_2 (ref. 45) was used rather than Weinbaum's value of 7.4962×10^{-11} meter (1.4166 bohrs). Hence an isolated H_2 molecule had an energy E_m of -5.0037×10^{-18} joule (-1.14779 hartrees) rather than Weinbaum's value of -5.0042×10^{-18} joule (-1.14790 hartrees) (ref. 43). The average interaction energy is found by averaging over nuclear configurations, which was facilitated by choosing the configurations shown in figures 1(a), (c), and (e). The other three configurations possessed a greater-than-equilibrium internuclear distance.

In all six configurations the intermolecular distance R_r was varied. It had values of 1.0, 1.1, 1.2, 1.3, 1.4, 1.5, 1.6, 1.8, 2.0, 2.5, 3.0, 3.5, and 4.0 bohrs (1 bohr = 5.29167×10^{-11} m).

Energy and Interaction Energy

To find the electronic energy of the H_2 - H complex, a Löwdin transformation was performed on the orbitals, resulting in orthogonalized orbitals. Formal orthogonalized valence-bond structures were formed, and the matrix elements of the Hamiltonian were found. An eigenvalue problem was then solved to obtain the electronic energy. The nuclear repulsion energy was added to the electronic energy to get the energy of the complex. The energies of isolated H and H_2 were subtracted from the energy of the

complex to yield the interaction energy. This entire procedure was repeated for different values for the orbital exponents to enable the three orbital exponents to be optimized by numerical methods. These steps are given in the following subsections.

Löwdin transformation. - The symmetric orthogonalization procedure of Löwdin (ref. 46) was applied to the χ_p. The overlap integral is

$$S_{pq} \equiv \int \chi_p(1)\chi_q(1)dv_1 \tag{2}$$

Let

$$w_{pq} \equiv \frac{\zeta_p + \zeta_q}{2} R_{pq} \tag{3}$$

where R_{pq} is the distance between protons p and q. If $\zeta_p = \zeta_q$, S_{pq} is given by Slater (ref. 47). If $\zeta_p \neq \zeta_q$,

$$S_{pq} = \frac{R_{pq}^3 \sqrt{\zeta_p^3 \zeta_q^3}}{4} \left[\frac{e^{\breve{q}} - e^{-\breve{q}}}{\breve{q}} \frac{2}{w_{pq}^2} \left(1 + w_{pq} + \frac{w_{pq}^2}{2}\right) + e^{-\breve{q}} \left(\frac{1}{\breve{q}} + \frac{2}{\breve{q}^2} + \frac{2}{\breve{q}^3}\right) \right.$$
$$\left. + e^{\breve{q}} \left(-\frac{1}{\breve{q}} + \frac{2}{\breve{q}^2} - \frac{2}{\breve{q}^3}\right) \right] \frac{e^{-w_{pq}}}{w_{pq}} \tag{4}$$

where

$$\breve{q} \equiv \frac{\zeta_p - \zeta_q}{2} R_{pq} \tag{5}$$

It is desired to find the Löwdin transformation matrix $\underline{\underline{M}}_\chi^{-1/2}$ such that

$$\underline{\chi}' = \underline{\chi}\underline{\underline{M}}_\chi^{-1/2} \tag{6}$$

where $\underline{\chi}$ is a row vector with elements χ_p, and $\underline{\chi}'$ is a row vector of the three orthogonalized orbitals χ_p'. First the eigenvalue problem

$$\widetilde{U}SU = d \tag{7}$$

is solved, where $\underline{S}$ is a matrix with elements S_{pq}. The matrix $\underline{d}$ is diagonal, with eigenvalues as diagonal elements. Thus

$$\underline{d}^{-1/2} = \begin{bmatrix} d_{11}^{-1/2} & 0 & 0 \\ 0 & d_{22}^{-1/2} & 0 \\ 0 & 0 & d_{33}^{-1/2} \end{bmatrix} \tag{8}$$

Finally,

$$\underline{M_\chi^{-1/2}} = \underline{U}\,\underline{d}^{-1/2}\,\widetilde{\underline{U}} \tag{9}$$

Use of equation (6) then accomplishes the Löwdin transformation to obtain $\underline{\chi}'$.

Formal orthogonalized valence-bond structures. - To produce the proper anti-symmetry, the χ_p' are combined in antisymmetrized products of orthogonalized spin orbitals.

$$(pq\bar{r}) = (3!)^{-1/2} \det\left[\chi_p'(1)\alpha(1),\ \chi_q'(2)\alpha(2),\ \chi_r'(3)\beta(3)\right] \tag{10}$$

where $\alpha(1)$ is the spin eigenfunction of electron 1 with the component of spin angular momentum along the axis of quantization equal to $\hbar/2$, and $\beta(3)$ is the spin eigenfunction of electron 3 with the component of spin angular momentum along the axis of quantization equal to $-\hbar/2$. The shorthand notation is given on the left side of equation (10), wherein a bar indicates β spin and no bar indicates α spin. To facilitate computing for some purposes, the $(pq\bar{r})$ are arranged in dictionary order in a three by three matrix (ref. 48):

$$\begin{bmatrix} (ab\bar{a}) & (ab\bar{b}) & (ab\bar{c}) \\ (ac\bar{a}) & (ac\bar{b}) & (ac\bar{c}) \\ (bc\bar{a}) & (bc\bar{b}) & (bc\bar{c}) \end{bmatrix} \tag{11}$$

For our purposes we will regard the $(pq\bar{r})$ as a nine-element row vector with the ele-

ments numbered down the first column in equation (11), then down the second column, etc. When numbered in this way, set

$$\varphi_i = (pq\bar{r}) \qquad i = 1, 2, \ldots, 9 \tag{12}$$

where p, q, and $\bar{r}$ are given in equation (11).

The formal orthogonalized valence-bond structures ψ_j are linear combinations of the φ_i. These ψ_j are eigenfunctions of the total electron spin with total spin quantum number of 1/2 and component of the total spin angular momentum along the axis of quantization of $\hbar/2$. These are obtained by temporarily putting a phantom orbit χ'_d at infinity as outlined by Pauling (ref. 49) and are

$$
\left.
\begin{aligned}
\psi_1 &= 2^{-1/2}(-\varphi_3 - \varphi_5) & \psi_5 &= \varphi_1 \\
\psi_2 &= 2^{-1/2}(-\varphi_3 + \varphi_7) & \psi_6 &= -\varphi_9 \\
\psi_3 &= -\varphi_2 & \psi_7 &= \varphi_4 \\
\psi_4 &= -\varphi_6 & \psi_8 &= \varphi_8
\end{aligned}
\right\} \tag{13}
$$

where formal singly polar structures are included. All ψ_i are orthonormal (see ref. 50) except ψ_1 and ψ_2. These may be made orthonormal by the Schmidt orthogonalization procedure, which results in replacing ψ_2 in equation (13) by a new ψ_2 such that

$$\psi_2 = 6^{-1/2}(-\varphi_3 + \varphi_5 + 2\varphi_7) \tag{14}$$

Equations (13) (excluding ψ_2) and (14) can be represented by

$$\underline{\psi} = \underline{\varphi} \, \underline{V} \tag{15}$$

where $\underline{V}$ is a nine by eight matrix. The wave function of the system was taken as

$$\Psi = \underline{\psi} \, \underline{C} \tag{16}$$

where $\underline{C}$ is a column vector determined by minimizing the electronic energy E_e. This is accomplished by the variation principle for orthonormal functions (ref. 51), which poses an eigenvalue problem.

$$\underline{H}\,\underline{C} = E_e\underline{C} \tag{17}$$

where the smallest of the several eigenvalues E_e is the ground state electronic energy and $\underline{H}$ is a matrix whose elements are given in the following sections.

Matrix elements of the Hamiltonian. - The Hamiltonian operator for the electronic energy in atomic units with the hartree as the unit of energy is

$$\hat{H} = \sum_{i=1}^{3} -\frac{1}{2}\nabla_i^2 + \sum_{i=1}^{3}\sum_{p=a}^{c} -\frac{1}{r_{pi}} + \sum_{i=2}^{3}\sum_{j=1}^{i-1}\frac{1}{r_{ij}} \tag{18}$$

Here ∇_i^2 is the Laplacian operator for the coordinates of electron i, and the p summation is over protons a, b, and c. The elements of the $\underline{H}$ matrix in equation (17) are then

$$H_{nk} = \int \psi_n^* \hat{H}\psi_k \, d\tau \tag{19}$$

where τ includes electron configuration and spin coordinates. From equations (15) and (19)

$$\underline{H} = \underline{\tilde{V}}H_\varphi\underline{V} \tag{20}$$

where

$$\left(H_\varphi\right)_{ij} = \int \varphi_i\hat{H}\varphi_j \, d\tau \tag{21}$$

The matrix elements $\left(H_\varphi\right)_{ij}$ can be found from Slater's rules (ref. 50 after correction of a typographical error) if two kinds of integrals are known.

$$\overline{F}_{ij} \equiv \int \chi_i'(1)\left(-\frac{1}{2}\nabla_1^2 + \sum_{p=a}^{c} -\frac{1}{r_{p1}}\right)\chi_j'(1)dv_1 \tag{22}$$

$$\overline{G}_{ijkl} \equiv \iint \chi'_i(1)\chi'_j(1)\chi'_k(2)\chi'_l(2)\frac{1}{r_{12}}dv_1\,dv_2 \tag{23}$$

where r_{12} is the distance from electron 1 to electron 2, dv_1 is the volume element for electron 1, and dv_2 is the volume element for electron 2. From equations (6), (22), and (23)

$$\overline{F}_{ij} = \sum_{k=1}^{3}\left(M_\chi^{-1/2}\right)_{ki}\sum_{l=1}^{3}\left(M_\chi^{-1/2}\right)_{lj}\left(K_{kl} + \sum_{p=a}^{c}L_{klp}\right) \tag{24}$$

$$\overline{G}_{ijkl} = \sum_{m=1}^{3}\left(M_\chi^{-1/2}\right)_{mi}\sum_{n=1}^{3}\left(M_\chi^{-1/2}\right)_{nj}\sum_{o=1}^{3}\left(M_\chi^{-1/2}\right)_{ok}\sum_{p=1}^{3}\left(M_\chi^{-1/2}\right)_{pl}G_{mnop} \tag{25}$$

where

$$K_{kl} \equiv \int \chi_k(1)\left(-\frac{1}{2}\nabla_1^2\right)\chi_l(1)dv_1 \tag{26}$$

$$L_{jkp} \equiv \int \chi_j(1)\chi_k(1)\left(\frac{-1}{r_{p1}}\right)dv_1 \tag{27}$$

$$G_{mnop} \equiv \iint \chi_m(1)\chi_n(1)\chi_o(2)\chi_p(2)\frac{1}{r_{12}}dv_1\,dv_2 \tag{28}$$

The methods of evaluating K_{kl}, L_{jkp}, and G_{mnop} are given by Patch (ref. 43).

Energies. - The energy E is the electronic energy plus the nuclear repulsion energy:

$$E = E_e + \frac{1}{R_{ab}} + \frac{1}{R_{ac}} + \frac{1}{R_{bc}} \tag{29}$$

10

The interaction energy E_{int} is the energy E minus the energies $E_m(r)$ and E_{at} of the isolated H_2 molecule with internuclear distance r and the isolated H atom, respectively:

$$E_{int} = E - E_m(r) - E_{at} \tag{30}$$

The diatomic internuclear distance used in equation (30) was the same as in the $H_2 - H$ complex (see fig. 1), and the corresponding $E_m(r)$ have been tabulated by Patch (ref. 43) for Weinbaum's covalent-ionic valence-bond model of H_2. Of course, E_{at} was -2.17972×10^{-18} joule (-0.5 hartree).

Optimization of orbital exponents. - To optimize the orbital exponents, it is necessary to solve the eigenvalue problem (eq. (17)) for a number of sets of orbital exponents. A least-squares fit is made to the resulting values of E_{int}, and the values of the orbital exponents that minimize E_{int} are found from the fit coefficients.

The simplest case involves isosceles configurations because by symmetry $\zeta_b = \zeta_c$ (see fig. 1(d)). If the optimum values ζ_{ao} and ζ_{bo} are known approximately, then a least-squares fit may be made.

$$E_{int} \approx W_o + W_1\zeta_a + W_2\zeta_b + W_{11}\zeta_a^2 + W_{22}\zeta_b^2 + W_{12}\zeta_a\zeta_b \tag{31}$$

where the E_{int} to be fit are calculated from equations (17), (29), and (30) for values $\zeta_a = \zeta_{ao} - \Delta\zeta$, ζ_{ao}, $\zeta_{ao} + \Delta\zeta$, and $\zeta_b = \zeta_{bo} - \Delta\zeta$, ζ_{bo}, $\zeta_{bo} + \Delta\zeta$ (nine sets of ζ_a and ζ_b). Here, $\Delta\zeta$ is an arbitrary number much smaller than ζ_{ao} or ζ_{bo}, and ζ_{ao} and ζ_{bo} are estimates. After the least-squares fit coefficients W have been found, the minimum of equation (31) can be found by direct calculation, yielding the true ζ_{ao} and ζ_{bo}.

The other case applies to linear and scalene configurations. Here, the optimum orbital exponents are generally all different so the least-squares fit is of the form

$$E_{int} \approx W_o + W_1\zeta_a + W_2\zeta_b + W_3\zeta_c + W_{11}\zeta_a^2 + W_{22}\zeta_b^2 + W_{33}\zeta_c^2 + W_{12}\zeta_a\zeta_b$$
$$+ W_{13}\zeta_a\zeta_c + W_{23}\zeta_b\zeta_c \tag{32}$$

where the E_{int} to be fit are calculated from equations (17), (29), and (30) for values $\zeta_a = \zeta_{ao} - \Delta\zeta$, ζ_{ao}, $\zeta_{ao} + \Delta\zeta$; $\zeta_b = \zeta_{bo} - \Delta\zeta$, ζ_{bo}, $\zeta_{bo} + \Delta\zeta$; $\zeta_c = \zeta_{co} - \Delta\zeta$, ζ_{co}, $\zeta_{co} + \Delta\zeta$ (27 sets of ζ_a, ζ_b, and ζ_c). The rest of the procedure is the same.

Average Interaction Energy

The average interaction energy $\overline{E}_{int}$ of an H_2 molecule and an H atom is, to a first approximation, the interaction energy for equilibrium diatomic internuclear distance averaged over all possible orientations of the H_2 molecule.

$$\overline{E}_{int} = \frac{1}{4\pi} \int_{4\pi} E_{int} \, d\Omega \tag{33}$$

where Ω is the solid angle for H_2 orientation.

Since only three configurations with equilibrium diatomic internuclear distances were considered in this report, an additional approximation was necessary. This was the truncated expansion of E_{int} in terms of Legendre polynomials Θ_i:

$$E_{int} = f_0 \Theta_0 (\cos \theta) + f_2 \Theta_2 (\cos \theta) + f_4 \Theta_4 (\cos \theta) \tag{34}$$

where the f's are expansion coefficients and θ is the angle between the internuclear axis of H_2 and the line through the H atom bisecting H_2. Odd Legendre polynomials were ruled out by symmetry. The result of substituting equation (34) into (33) is

$$\overline{E}_{int} = \frac{1}{15} E_{int,A} + \frac{8}{15} E_{int,C} + \frac{2}{5} E_{int,E} \tag{35}$$

Electric Dipole Moment

Calculation of the dipole moment requires an electron population analysis in terms of the original nonorthogonal orbitals χ_p. A column vector $\underline{C}'$ may be defined by

$$\Psi = \underline{\varphi} \, \underline{C}' \tag{36}$$

From equations (15), (16), and (36)

$$\underline{C}' = \underline{V} \underline{C} \tag{37}$$

The electron population in the orbital density $\chi'_m \chi'_n$ irrespective of spin state is (ref. 41)

12

$$P'_{mn} = \sum_{r=1}^{9} C'_r \sum_{s=1}^{9} C'_s \left(n_{rs}^{m\alpha n\alpha} + n_{rs}^{m\beta n\beta} \right) \tag{38}$$

where $n_{rs}^{m\alpha n\alpha}$ and $n_{rs}^{m\beta n\beta}$ are coefficients of spin-orbital products and are called $n_{rs}^{\mu\nu}$ by Magnasco and Musso (refs. 41 and 48), who also give rules for evaluating them (ref. 48).

The electron population in the orbital density $\chi_p\chi_q$ irrespective of spin state is (ref. 41)

$$P_{pq} = \sum_{m=1}^{3} \left(M_\chi^{-1/2} \right)_{pm} \sum_{n=1}^{3} P'_{mn} \left(M_\chi^{-1/2} \right)_{qn} \tag{39}$$

The normalized 1-electron population is

$$\mathscr{P}_{pq} = P_{pq} S_{pq} \tag{40}$$

where the three diagonal elements of the matrix $\underline{\mathscr{P}}$ give the atomic populations and the off-diagonal elements give the overlap populations. For instance, the population in the overlap between orbitals centered on protons a and b is $\mathscr{P}_{ab} + \mathscr{P}_{ba}$. The elements of the $\underline{\mathscr{P}}$ matrix, of course, add to three, the number of electrons.

To find the dipole moment from $\underline{\mathscr{P}}$, it is necessary to know locations of the atomic charge centers and the overlap charge centers. Cartesian coordinates with the origin one-third of the way from the molecule toward the atom were chosen (see fig. 1(a)). The jth Cartesian coordinate of either type of charge center was designated C_{pqj}, where p and q correspond to the two orbitals χ_p and χ_q involved in an overlap charge or where p and q are equal and correspond to the one orbital involved in an atomic charge. The $\overline{C}_{ppj}$ for atomic charges are, of course, identical to the coordinates of the protons C_{pj}. For overlap charges

$$\overline{C}_{pqj} = \left(\frac{1}{2} - \Delta_{pq} \right) C_{pj} + \left(\frac{1}{2} + \Delta_{pq} \right) C_{qj} \tag{41}$$

where Δ_{pq} is the displacement of the overlap charge center from the p - q geometric center, measured in the direction from p towards q and expressed in units of R_{pq}. If $\zeta_p = \zeta_q$, $\Delta_{pq} = 0$ by symmetry. If $\zeta_p \neq \zeta_q$,

13

$$\Delta_{pq} = \frac{R_{pq}^3 e^{-w_{pq}}}{8S_{pq}w_{pq}^2} \sqrt{\zeta_p^3 \zeta_q^3} \left\{ \left[e^{-\breve{q}}\left(-\frac{1}{\breve{q}} - \frac{1}{\breve{q}^2}\right) - e^{\breve{q}}\left(\frac{1}{\breve{q}} - \frac{1}{\breve{q}^2}\right)\right] \left(\frac{6}{w_{pq}^2} + \frac{6}{w_{pq}} + 3 + w_{pq}\right) \right.$$

$$\left. + \left[e^{-\breve{q}}\left(\frac{1}{\breve{q}} + \frac{3}{\breve{q}^2} + \frac{6}{\breve{q}^3} + \frac{6}{\breve{q}^4}\right) + e^{\breve{q}}\left(\frac{1}{\breve{q}} - \frac{3}{\breve{q}^2} + \frac{6}{\breve{q}^3} - \frac{6}{\breve{q}^4}\right) \right] (1 + w_{pq}) \right\} \qquad (42)$$

The jth component of the dipole moment in atomic units is then

$$\mu_j = -\sum_{p=1}^{3}\sum_{q=1}^{3} \mathscr{P}_{pq}\overline{C}_{pqj} \qquad (43)$$

By symmetry, only the x and z components may be nonzero.

Computer Program

All calculations including optimizing the orbital exponents were done by one FORTRAN IV IBM version-13 program for an IBM 7094 digital computer. To obtain a set of optimized orbital exponents, interaction energy, and dipole moment, the running times were 4.5, 8.7, and 2.1 minutes for the linear, scalene, and isosceles configurations, respectively.

RESULTS AND DISCUSSION

In this section values for the orbital exponents, interaction energy, average interaction energy, dipole moment, and dipole moment derivative are given and compared with the results of other investigators.

Orbital Exponents and Interaction Energy

In optimizing the orbital exponents, it was found that the estimates had to be fairly accurate for the coefficients of equation (31) or (32) to give meaningful values for the op-

14

TABLE II. - AVERAGE INTERACTION ENERGY

FOR $H_2 + H$

Intermolecular distance, R_r		Average interaction energy, $\overline{E}_{int}$	
m	bohr	J	hartree
5.29167×10^{-11}	1.0	2.5712×10^{-18}	0.58980
5.82084	1.1	2.0969	.48100
6.35000	1.2	1.7730	.40670
6.87917	1.3	1.4969	.34336
7.40834	1.4	1.2400	.28445
7.93751	1.5	1.0374	.23797
8.46667	1.6	0.8753	.20079
9.52501	1.8	.6367	.14605
1.05833×10^{-10}	2.0	.4732	.10854
1.32292	2.5	.2353	.05398
1.58750	3.0	.1173	.02690
1.85208	3.5	.0569	.01305
2.11667	4.0	.0267	.00613
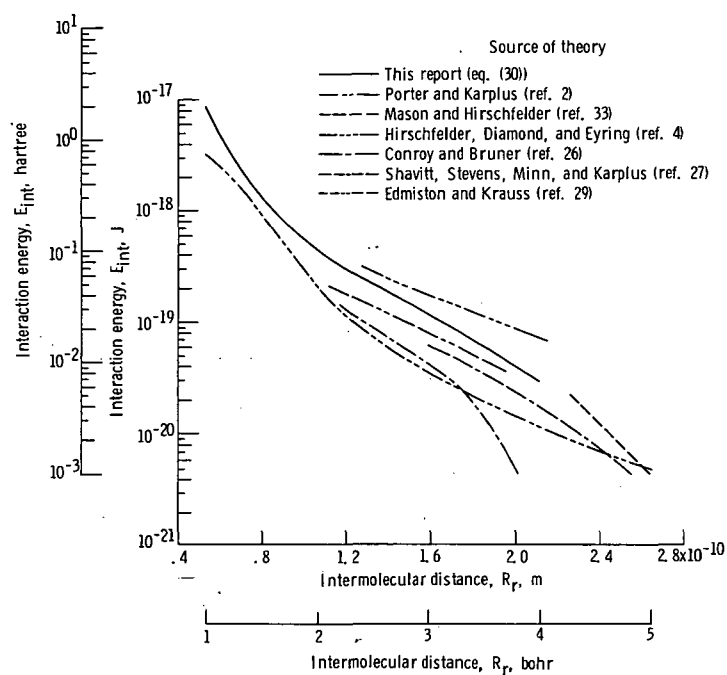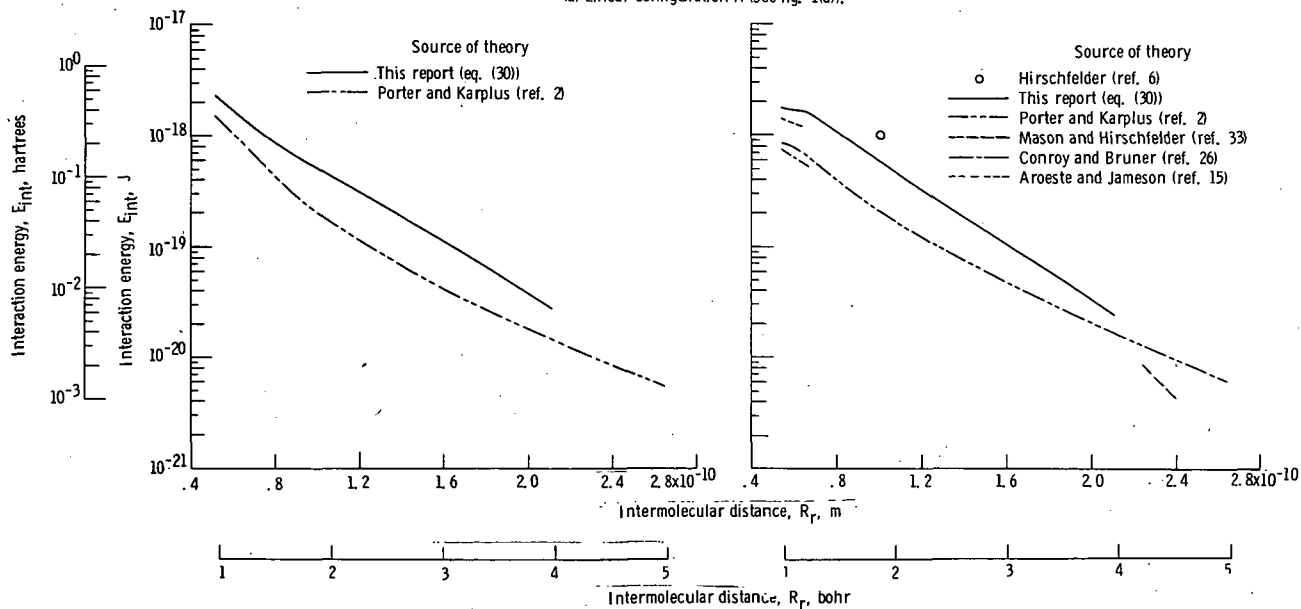
Figure 2. – Interaction energy for three configurations of a hydrogen molecule and a hydrogen atom, each configuration having equilibrium inter-nuclear distance in the molecule.

16

timum orbital exponents. Consequently, before running the program in the mode for automatic least-squares fit to E_{int} and optimization of ζ_i, it was run in another mode that allowed one ζ_i to be varied at a time, and the resulting E_{int}'s were hand plotted. In this way good estimates for the ζ_i were eventually obtained, allowing the program to be run in the automatic-fit mode. In some cases the automatic-fit mode had to be repeated with progressively smaller $\Delta\zeta$ until a $\Delta\zeta$ of 1.89×10^8 reciprocal meters (0.01 bohr^{-1}) ran successfully, producing optimum ζ_i's that fell within the ζ_i grid used to obtain the least-squares fit for that run. The final orbital exponents and interaction energy are given in table I for 3 nuclear configurations and 13 intermolecular distances. The apparent discontinuity at $R_r = 6.422\times10^{-11}$ meter (1.2136 bohrs) for orbital exponents of configuration E (isosceles) is due to a change of symmetry of the eigenfunction as the isosceles triangle goes through the equilateral triangle configuration.

The interaction energies are plotted in figures 2(a), (b), and (c) for configurations A, C, and E. The change of symmetry mentioned produces a slight Jahn-Teller cusp in the interaction energy of configuration E. For all configurations, the interaction energy increases monotonically as R_r is decreased. For large R_r the order of increasing interaction energy is configurations E, C, and A. For small R_r the linear configuration A has the highest interaction energy. For intermediate R_r it is difficult to generalize.

Average Interaction Energy

The average interaction energy is given in table II and plotted in figure 3. It increases monotonically as R_r decreases.

Electric Dipole Moment and Its Derivative

The components of the electric dipole moments for configurations A, C, and E are given in table III for 13 intermolecular distances. They are plotted in figure 4. Again, there is an apparent discontinuity due to the change of symmetry as the isosceles configuration goes through the equilateral triangle configuration. The x-component of the dipole moment for configurations A and E is zero by symmetry.

To obtain the derivatives of the components of the electric dipole moment with respect to the H_2 internuclear distance, all calculations were repeated for a greater-than-equilibrium internuclear distance (configurations B, D, and F of fig. 1). The derivatives were found from the approximation $\partial\mu_i/\partial r \approx \Delta\mu_i/\Delta r$. The results are given in table III and plotted in figure 5. There is the usual apparent discontinuity for the isosceles configuration.

TABLE I. – ENERGY AND ORBITAL EXPONENTS FOR H_2 + H

| Intermolecular distance, R_r		Configuration[a]	Orbital exponent, ζ_a		Orbital exponent, ζ_b		Orbital exponent, ζ_c		Interaction energy, E_{int}	
m	bohr		1/m	1/bohr	1/m	1/bohr	1/m	1/bohr	J	hartree
5.29167×10^{-11}	1.0	A	2.4966×10^{10}	1.32113	-3.7651×10^{10}	1.99239	1.8262×10^{10}	0.96636	8.7946×10^{-18}	2.01737
		C	2.4421	1.29230	3.1230	1.65260	1.8172	.96159	2.3052	0.52878
		E	3.1118	1.64667	1.9325	1.02262	1.9325	1.02262	1.8885	.43321
5.82084×10^{-11}	1.1	A	2.4870×10^{10}	1.31605	3.6068×10^{10}	1.90860	1.8652×10^{10}	0.98700	5.5201×10^{-18}	1.26625
		C	2.3651	1.25154	3.0987	1.63971	1.8481	.97796	1.8935	0.43434
		E	3.0355	1.60630	1.9094	1.01037	1.9094	1.01037	1.7975	.41233
6.35000×10^{-11}	1.2	A	2.4567×10^{10}	1.30003	3.4497×10^{10}	1.82548	1.8951×10^{10}	1.00284	3.6986×10^{-18}	0.84841
		C	2.2972	1.21560	3.0642	1.62145	1.8765	0.99298	1.5612	.35811
		E	2.9606	1.56663	1.8866	0.99831	1.8866	.99831	1.7344	.39786
6.87917×10^{-11}	1.3	A	2.4145×10^{10}	1.27769	3.3139×10^{10}	1.75359	1.9199×10^{10}	1.01596	2.5893×10^{-18}	0.59395
		C	2.2364	1.18341	3.0197	1.59791	1.9039	1.00749	1.2967	.29744
		E	1.7928	0.94870	2.3230	1.22928	2.3230	1.22928	1.5816	.36281
7.40834×10^{-11}	1.4	A	2.3658×10^{10}	1.25189	3.1988×10^{10}	1.69272	1.9416×10^{10}	1.02742	1.8747×10^{-18}	0.43003
		C	2.1818	1.15454	2.9724	1.57288	1.9294	1.02100	1.0868	.24930
		E	1.8188	0.96243	2.3199	1.22763	2.3199	1.22763	1.3386	.30705
7.93751×10^{-11}	1.5	A	2.3146×10^{10}	1.22481	3.1002×10^{10}	1.64052	1.9612×10^{10}	1.03780	1.3964×10^{-18}	0.32032
		C	2.1334	1.12894	2.9216	1.54600	1.9537	1.03382	9.1962×10^{-19}	.21095
		E	1.8344	0.97072	2.3177	1.22647	2.3177	1.22647	1.1346×10^{-18}	.26026
8.46667×10^{-11}	1.6	A	2.2639×10^{10}	1.19799	3.0136×10^{10}	1.59469	1.9794×10^{10}	1.04744	1.0672×10^{-18}	0.24481
		C	2.0912	1.10657	2.8681	1.51773	1.9768	1.04607	7.8522×10^{-19}	.18012
		E	1.8444	0.97600	2.3155	1.22530	2.3155	1.22530	9.6348	.22101
9.52501×10^{-11}	1.8	A	2.1708×10^{10}	1.14871	2.8651×10^{10}	1.51611	2.0133×10^{10}	1.06535	6.6961×10^{-19}	0.15360
		C	2.0241	1.07111	2.7571	1.45896	2.0210	1.06944	5.8578	.13437
		E	1.8582	0.98332	2.3093	1.22200	2.3093	1.22200	6.9912	.16037
1.05833×10^{-10}	2.0	A	2.0940×10^{10}	1.10808	2.7389×10^{10}	1.44931	2.0455×10^{10}	1.08239	4.5787×10^{-19}	0.10503
		C	1.9782	1.04678	2.6475	1.40097	2.0638	1.09209	4.4641	.10240
		E	1.8673	0.98813	2.3020	1.21812	2.3020	1.21812	5.1136	.11730
1.32292×10^{-10}	2.5	A	1.9774×10^{10}	1.04637	2.4945×10^{10}	1.32001	2.1268×10^{10}	1.12541	2.2612×10^{-19}	0.05187
		C	1.9252	1.01876	2.4308	1.28630	2.1625	1.14432	2.3275	.05339
		E	1.8844	0.99714	2.2849	1.20908	2.2849	1.20908	2.4029	.05512
1.58750×10^{-10}	3.0	A	1.9314×10^{10}	1.02201	2.3544×10^{10}	1.24587	2.1983×10^{10}	1.16326	1.2180×10^{-19}	0.02794
		C	1.9101	1.01077	2.3260	1.23083	2.2240	1.17686	1.1875	.02724
		E	1.8942	1.00237	2.2749	1.20382	2.2749	1.20382	1.1452	.02627
1.85208×10^{-10}	3.5	A	1.9125×10^{10}	1.01204	2.2973×10^{10}	1.21567	2.2382×10^{10}	1.18440	6.2427×10^{-20}	0.01432
		C	1.9037	1.00737	2.2884	1.21093	2.2500	1.19065	5.8286	.01337
		E	1.8970	1.00381	2.2706	1.20155	2.2706	1.20155	5.4057	.01240
2.11667×10^{-10}	4.0	A	1.9029×10^{10}	1.00696	2.2781×10^{10}	1.20548	2.2554×10^{10}	1.19347	3.0254×10^{-20}	0.00694
		C	1.8990	1.00491	2.2756	1.20415	2.2604	1.19613	2.7552	.00632
		E	1.8960	1.00328	2.2690	1.20070	2.2690	1.20070	2.5023	.00574

[a]See fig. 1.
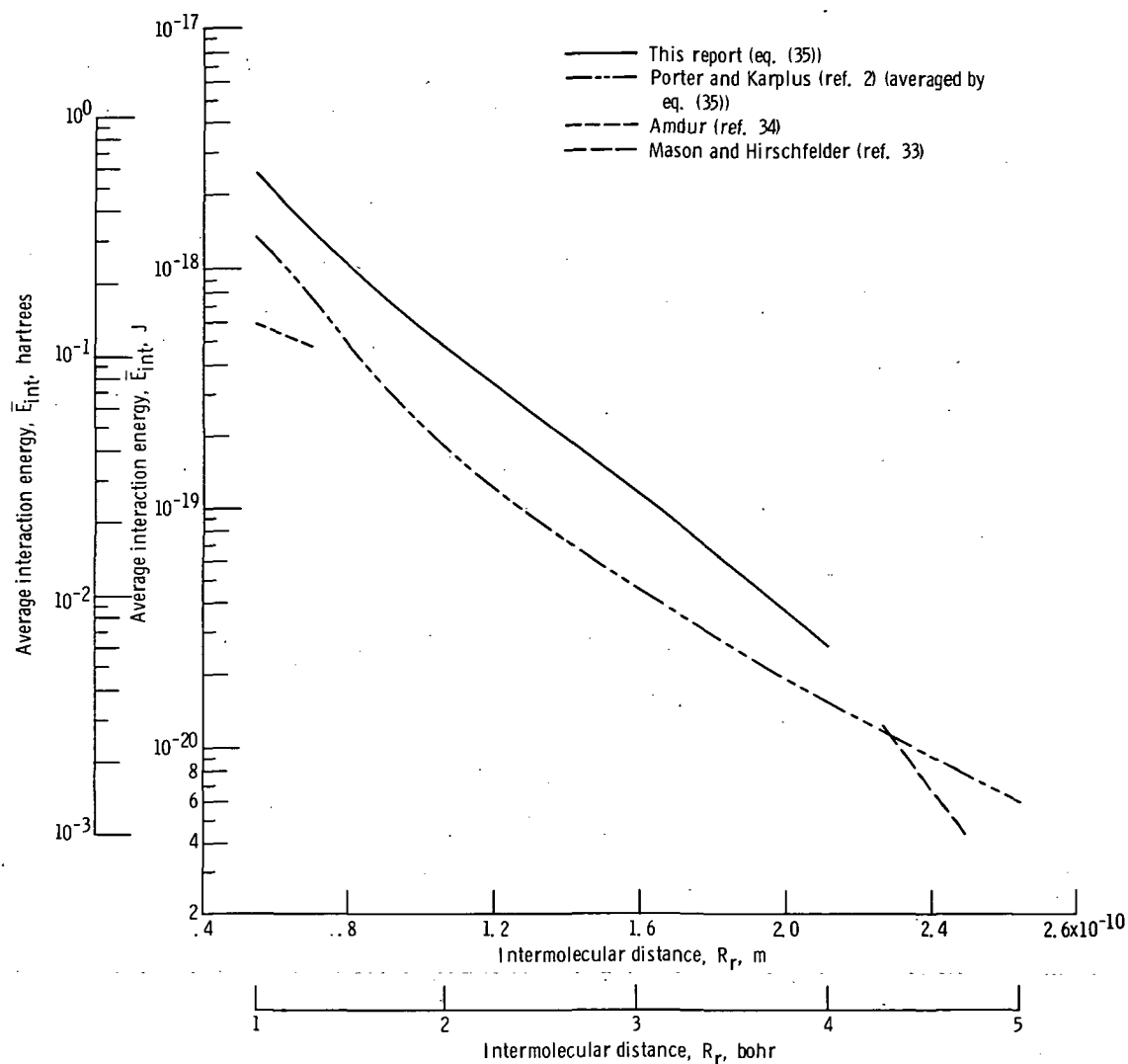
Figure 3. - Average interaction energy for a hydrogen molecule and a hydrogen atom. For the curve labelled "This report" the molecule had an internuclear distance of 7.41599×10^{-11} meter (1.401446 bohr).

| Intermolecular distance, R_r		Configuration[a]	Component of dipole moment, μ_x		Component of dipole moment, μ_z		Derivative of component of dipole moment, $\partial\mu_x/\partial r$		Derivative of component of dipole moment, $\partial\mu_z/\partial r$	
m	bohr		C-m	at. units	C-m	at. units	C	at. units	C	at. units
5.29167×10^{-11}	1.0	A	0	0	2.67638×10^{-30}	0.315693	0	0	-2.595×10^{-20}	-0.1620
		C	1.81431×10^{-30}	.214008	2.80947	.331392	$.823\times10^{-20}$	.0514	-1.554	-.0970
		E	0	0	2.12124	.250212	0	0	-1.352	-.0844
5.82084×10^{-11}	1.1	A	0	0	2.34716×10^{-30}	0.276860	0	0	-2.719×10^{-20}	-0.1697
		C	1.69238×10^{-30}	.199625	2.52880	.298285	1.203×10^{-20}	.0751	0.003	.0002
		E	0	0	2.48750	.293414	0	0	-2.022	-.1262
6.35000×10^{-11}	1.2	A	0	0	2.09418×10^{-30}	0.247020	0	0	-2.113×10^{-20}	-0.1319
		C	1.57656×10^{-30}	.185964	2.17885	.257007	1.405×10^{-20}	.0877	1.774	.1107
		E	0	0	2.85553	.336825	0	0	-2.494	-.1557
6.87917×10^{-11}	1.3	A	0	0	1.85676×10^{-30}	0.219015	0	0	-1.032×10^{-20}	-0.0644
		C	1.45789×10^{-30}	.171966	1.77748	.209663	1.762×10^{-20}	.1100	3.571	.2229
		E	0	0	-4.18773	-.493965	0	0	1.956	.1221
7.40834×10^{-11}	1.4	A	0	0	1.61116×10^{-30}	0.190045	0	0	0.178×10^{-20}	0.0111
		C	1.34361×10^{-30}	.158486	1.34934	.159162	1.964×10^{-20}	.1226	5.120	.3196
		E	0	0	-3.95336	-.466320	0	0	1.182	.0738
7.93751×10^{-11}	1.5	A	0	0	1.35294×10^{-30}	0.159586	0	0	1.354×10^{-20}	0.0845
		C	1.23119×10^{-30}	.145225	9.18763×10^{-31}	.108373	2.107×10^{-20}	.1315	6.263	.3909
		E	0	0	-3.75114×10^{-30}	-.442467	0	0	0.644	.0402
8.46667×10^{-11}	1.6	A	0	0	1.08738×10^{-30}	0.128262	0	0	2.378×10^{-20}	0.1484
		C	1.12113×10^{-30}	.132243	5.08998×10^{-31}	.060039	2.185×10^{-20}	.1364	6.919	.4319
		E	0	0	-3.55798×10^{-30}	-.419683	0	0	0.364	.0227
9.52501×10^{-11}	1.8	A	0	0	5.74480×10^{-31}	0.067763	0	0	3.685×10^{-20}	0.2300
		C	9.11158×10^{-31}	.107476	-1.76507	-.020820	2.148×10^{-20}	.1341	6.825	.4260
		E	0	0	-3.14938×10^{-30}	-.371486	0	0	-0.328	-.0205
1.05833×10^{-10}	2.0	A	0	0	1.56746×10^{-31}	0.018489	0	0	3.872×10^{-20}	0.2417
		C	7.19679×10^{-31}	.084890	-6.21218	-.073276	1.913×10^{-20}	.1194	5.466	.3412
		E	0	0	-2.71693×10^{-30}	-.320476	0	0	-0.692	-.0432
1.32292×10^{-10}	2.5	A	0	0	-2.47144×10^{-31}	-0.029152	0	0	2.075	0.1295
		C	3.47420×10^{-31}	.040980	-8.27457	-.097603	1.043×10^{-20}	.0651	1.804	.1126
		E	0	0	-1.66838×10^{-30}	-.196794	0	0	-0.838	-.0523
1.58750×10^{-10}	3.0	A	0	0	-1.59772×10^{-31}	-0.018846	0	0	1.237	0.0772
		C	1.46979×10^{-31}	.017337	-5.31294	-.062669	$.418\times10^{-20}$	.0261	0.535	.0334
		E	0	0	-9.12345	-.107616	0	0	-.546	-.0341
1.85208×10^{-10}	3.5	A	0	0	-6.15572×10^{-32}	-0.007261	0	0	0.907	0.0566
		C	6.44396×10^{-32}	.007601	-2.79674×10^{-31}	-.032989	$.165\times10^{-20}$	.0103	.282	.0176
		E	0	0	-4.75036	-.056033	0	0	-.279	-.0174
2.11667×10^{-10}	4.0	A	0	0	-2.06773×10^{-32}	-0.002439	0	0	0.594	0.0371
		C	3.05200×10^{-32}	-.003600	-1.41019×10^{-31}	-.016634	$.069\times10^{-20}$	.0043	.179	.0112
		E	0	0	-2.43143	-.028680	0	0	-.130	-.0081

[a]See fig. 1.

20
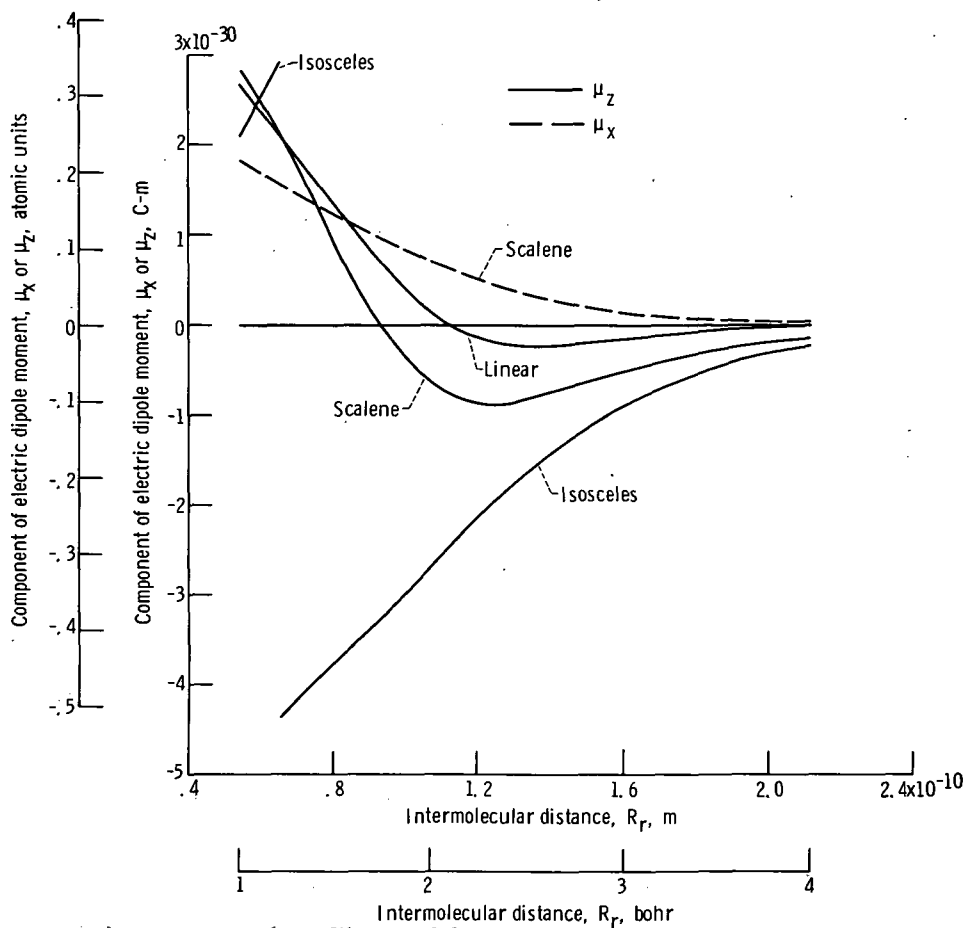
Figure 4. - Components of electric dipole moment for three configurations of a hydrogen molecule and a hydrogen atom. Coordinates are shown in figure 1(a). Components not shown are zero.
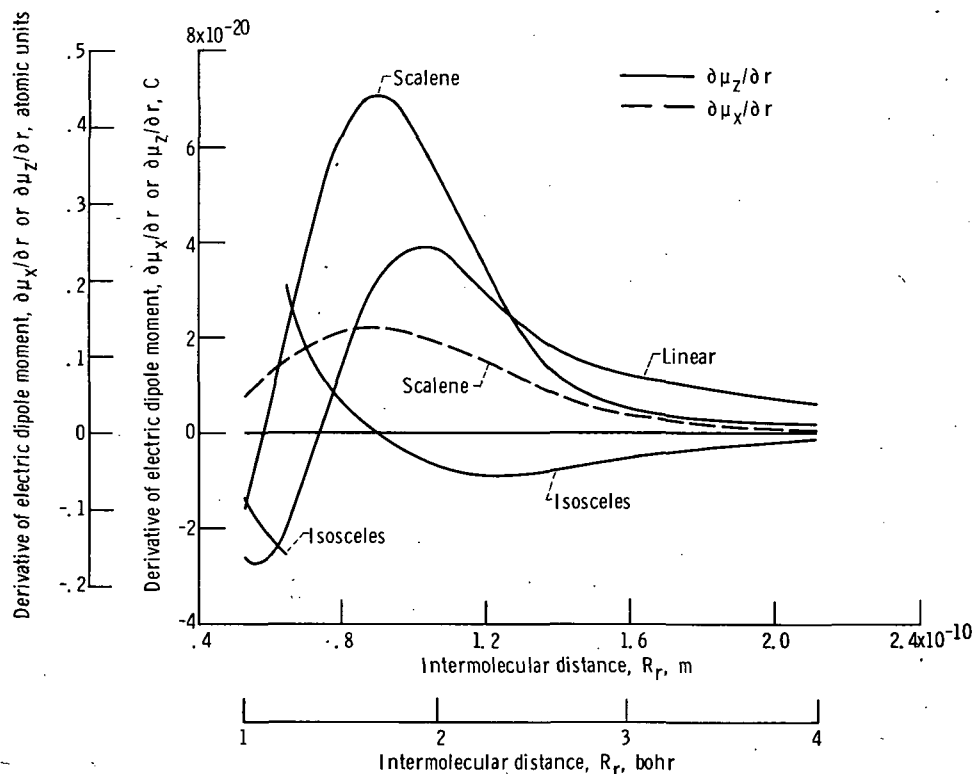
21

Figure 5. - Derivatives of electric dipole moment with respect to molecular internuclear distance for three configurations of a hydrogen molecule and a hydrogen atom. Coordinates are shown in figure 1(a). Derivatives not shown are zero.

Comparison with Other Investigators

The accuracy of the molecular integrals was checked against Magnasco and Musso (refs. 41 and 42) among others. Comparison of the values of energy, average interaction energy, dipole moment, and dipole moment derivative with values of other investigators is made in the following subsections.

Energy. - The energy of H_2 - H or H_3 has been calculated by a great many investigators. However, many of them used inaccurate molecular integrals. Others used over-simplified models. The most convincing check of the present calculation was made with a special linear symmetric configuration of Shavitt, Stevens, Minn, and Karplus (ref. 27, table XI). Their model was the same as in this report except that they may not have used orthogonalized orbitals. They used a ζ_b of 2.27149×10^{10} reciprocal meters (1.202 1/bohr) and $\zeta_a = \zeta_c$ of 1.99937×10^{10} reciprocal meters (1.058 1/bohr). They got an energy of -7.0213×10^{-18} joule (-1.6106 hartrees), which is exactly what the method of this report gave.

A comparison of interaction energies for the linear configurations of this report

22

$(r \approx 7.41 \times 10^{-11}$ m (1.40 bohrs)) is made with other investigators in figure 2(a). The energies of Hirschfelder, Diamond, and Eyring (ref. 4) are higher than this report because they used the same value of orbital exponent for all three Slater-type 1s orbitals. The energies of Conroy and Bruner (ref. 26) are lower, presumably because they included electron correlation in their wavefunction in a more realistic manner. The energies of Shavitt, Stevens, Minn, and Karplus (ref. 27) are lower than this report because they used 15 Slater-type orbitals rather than three. The energies of Edmiston and Krauss (ref. 29) are lower than this report presumably because their molecular-orbital wave function, constructed from 36 s- and p-type Gaussian orbitals, was closer to the true wave function. In addition, two semiempirical calculations have been included, although a comparison with ab initio calculations is not entirely fair. The Porter and Karplus potential (ref. 2) correlates exchange reaction rates and trajectories fairly well (refs. 36 and 38) and is presumably realistic at intermolecular distances less than 1.75×10^{-10} meter (3.3 bohrs). The Mason and Hirschfelder potential (ref. 33) is the sum of a first-order perturbation energy and two dispersion terms and is presumably realistic for intermolecular distances greater than 2.65×10^{-10} meter (5 bohrs).

A comparison of interaction energies for the scalene configurations is made in figure 2(b). The Porter and Karplus potential (ref. 2) is again lower than the interaction energy calculated in this report.

A comparison of interaction energies for the isosceles configurations of this report $(r \approx 7.41 \times 10^{-11}$ m (1.40 bohrs)) is made with other investigators in figure 2(c) Hirschfelder's energy (ref. 6) is higher than this report because he assumed all Slater-type 1s orbitals to have orbital exponents of 1.88976×10^{10} reciprocal meters (1.0 1/bohr). Conroy and Bruner's energies (ref. 26) are lower, presumably because they included electron correlation in their wavefunction in a more realistic manner. Aroeste and Jameson's energies (ref. 15) are lower than this report, presumably because they approximated some molecular integrals. Trivedi's results (ref. 31) are not shown because of only one-place accuracy for some of his three-center molecular integrals and other errors. The semiempirical potentials of Porter and Karplus (ref. 2) and Mason and Hirschfelder (ref. 33) are also shown.

Average interaction energy from this report is compared with other investigators in figure 3. The semiempirical potential of Porter and Karplus (ref. 2) was averaged over H_2 orientations by use of equation (35) and is lower than this report because their potential was lower for each configuration. The semiempirical potential of Mason and Hirschfelder (ref. 33) was averaged by means of the approximation

$$\overline{E}_{int} = \frac{1}{3} E_{int,A} + \frac{2}{3} E_{int,E} \tag{44}$$

which is fully analogous to equation (35). The interaction energy obtained by Amdur (ref. 34) from scattering of an H atom beam in H_2 gas is the lowest of all for small intermolecular distances.

In summary, the interaction energy in this report is within the scatter of other ab initio calculations and has the proper dependence on intermolecular distance. At small intermolecular distances the dependence on H_2 orientation agrees with the Porter and Karplus potential (ref. 2). (It does not contradict Conroy and Bruner's finding (ref. 26) that the path of minimum energy involves a linear symmetric configuration because we fixed the H_2 internuclear distance at 7.41599×10^{-11} m (1.401446 bohrs), but their saddle-point in their minimum energy path occurs for H_2 internuclear distance of 9.26047 $\times 10^{-11}$ m (1.75 bohrs).) At large intermolecular distances the dependence of interaction energy on H_2 orientation agrees with the Mason and Hirschfelder potential (ref. 33). In any case, the interaction energy is a sensitive function of the model used because it is a small difference between two large numbers (the first number being H_3 energy and the second being the sum of isolated H_2 and isolated H energies).

Dipole moment and its derivative. - There are no previous calculations of either of these quantities themselves, but for large enough intermolecular distance accurate results may be obtained by classical methods: the H_2 quadrupole moment induces a dipole in the H atom. To draw meaningful conclusions from such a comparison, the components of the dipole moment should be expanded in normalized Legendre polynomials or normalized associated Legendre functions as follows:

$$\mu_z = \sum_l C_l(R_r)\Theta_l(\cos\theta) \tag{45}$$

$$2^{-1/2}(\mu_x + i\mu_y) = \sum_l \sum_m G_{lm}(R_r)\Theta_{lm}(\cos\theta)e^{im\Phi} \tag{46}$$

where θ and Φ are shown in figure 6. In atomic units the classical method gives

$$\left. \begin{array}{c} C_0 = 0 \\[2ex] C_2 = 3 \cdot (2/5)^{1/2}\, \alpha\, Q/R_r^4 \\[2ex] C_4 = 0 \\[2ex] G_{21} = -(6/5)^{1/2}\, \alpha\, Q/R_r^4 \end{array} \right\} \tag{47}$$
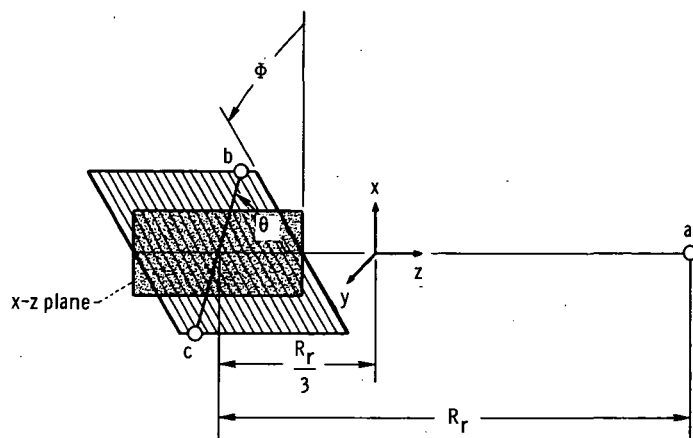
24

Figure 6. – Both sets of coordinates used in H_2-H collisions. The polar angle θ is measured from the z axis. The azimuthal angle Φ is measured from the x-z plane.
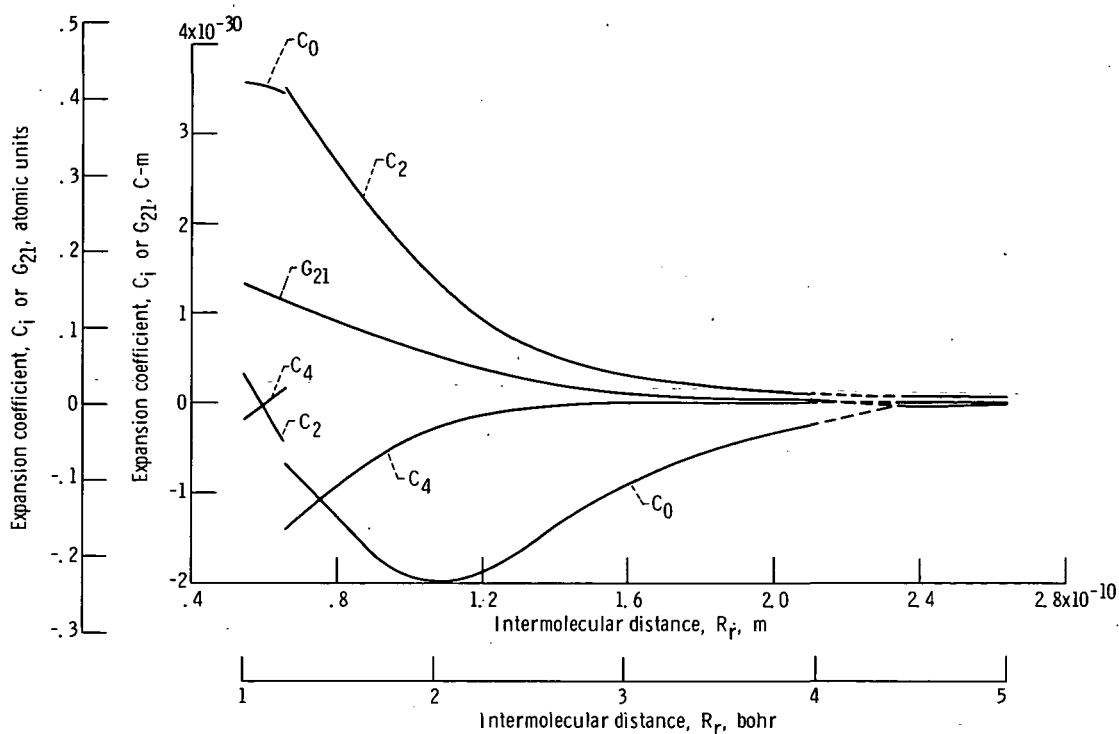

Figure 7. – Expansion coefficients of components of dipole moment for $H_2 + H$. Valence bond values are plotted from 1 to 4 bohr. Quadrupole induced values are plotted from 4.5 to 5 bohr. Dashed lines connecting corresponding coefficients were added from 4 to 4.5 bohr for clarity.

where α is the polarizability of the H atom and Q is the scalar quadrupole moment of H_2. The value of α has been given by Pauling and Wilson (ref. 52), and the value of Q by Kolos and Wolniewicz (ref. 53), who use a different definition so that their values must be divided by two. The results are plotted for R_r of 2.38×10^{-10} to 2.65×10^{-10} meter (4.5 to 5 bohrs) in figure 7. For comparison, the valence-bond results in figure 4 were expanded by equations (45) and (46) and plotted in figure 7 for R_r of 0.53×10^{-10} to 2.12×10^{-10} meter (1 to 4 bohrs). The valance-bond C_0 and C_4 correctly approach 0 as R_r becomes large. The valence-bond C_2 is in good agreement with the classical C_2. However, there is a minor difficulty in the case of G_{21}: at large R_r the valence-bond and classical values differ in sign, although both are small. This is because the 1s orbital centered on H in the valance-bond model cannot be polarized in the x direction. At smaller R_r x-polarization of H will be approximated by changes in orbital populations.

The derivatives of the components of dipole moment with respect to H_2 internuclear distance can be examined the same way. First they are expanded

$$\frac{\partial \mu_z}{\partial r} = \sum_{l} D_l(R_r) \Theta_l (\cos \theta) \tag{48}$$

$$\frac{\partial}{\partial r}\left[2^{-1/2}(\mu_x + i\mu_y) \right] = \sum_{l} \sum_{m} J_{lm}(R_r)\Theta_{lm}(\cos \theta)e^{im\Phi} \tag{49}$$

In atomic units the classical method gives

$$\left.\begin{aligned} D_0 &= 0 \\ D_2 &= 3 \cdot (2/5)^{1/2}\alpha Q'/R_r^4 \\ D_4 &= 0 \\ J_{21} &= -(6/5)^{1/2}\alpha Q'/R_r^4 \end{aligned}\right\} \tag{50}$$

where Q' is the derivative of Q with respect to H_2 internuclear distance. The results are plotted for R_r of 2.38×10^{-10} to 2.65×10^{-10} meter (4.5 to 5 bohrs) in figure 8. For comparison, the valence-bond results in figure 5 were expanded and plotted in figure 8 for R_r of 0.53×10^{-10} to 2.12×10^{-10} meter (1 to 4 bohrs). The valence-bond D_0 and D_4 correctly approach 0 for large R_r. The valence-bond D_2 is in excellent
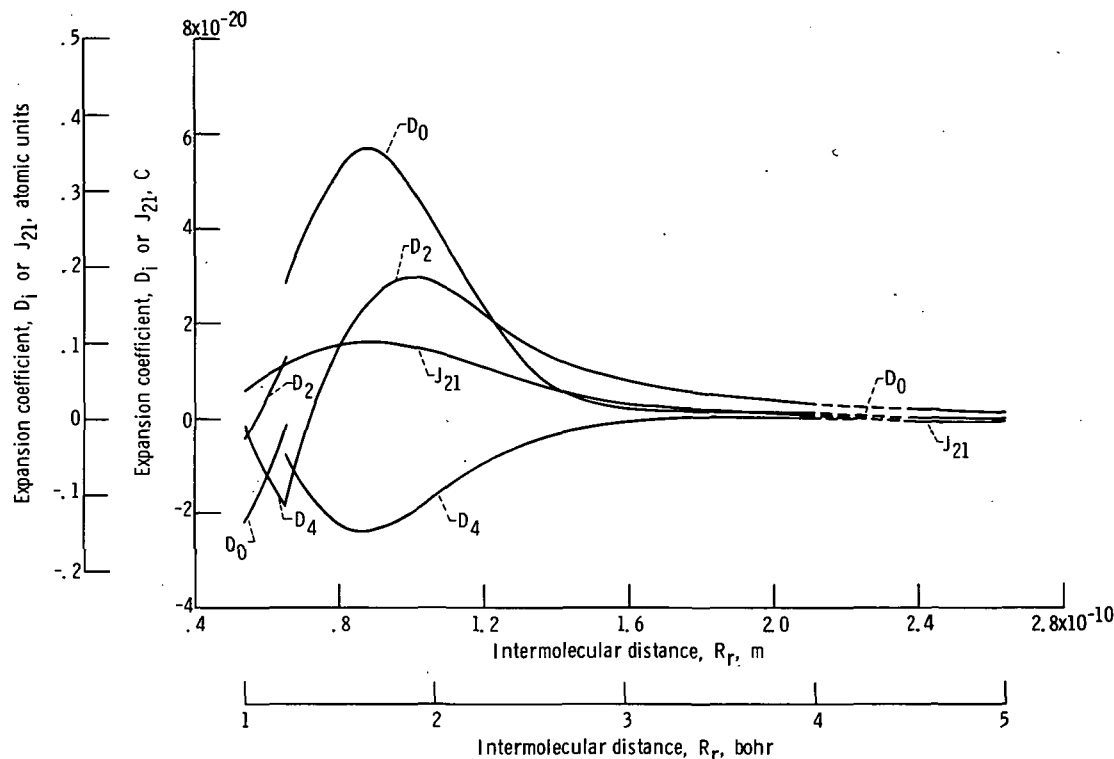
Figure 8. – Expansion coefficients of derivatives of components of dipole moment for H_2-H. Valence bond values are plotted from 1 to 4 bohr. Quadrupole induced values are plotted from 4.5 to 5 bohr. Dashed lines connecting corresponding coefficients were added from 4 to 4.5 bohr for clarity.

agreement with the classical D_2. However, for the reasons mentioned in the previous paragraph, the valence-bond J_{21} and classical J_{21} have different signs at large R_r. Fortunately they are both small.

CONCLUDING REMARKS

Full valence-bond ab initio calculations of molecular hydrogen-atomic hydrogen (H_2-H) interaction energy and electric dipole moment were carried out with accurate values for all molecular integrals and optimization of each orbital exponent. Linear, scalene, and isosceles configurations were included with intermolecular distances from 0.53×10^{-10} to 2.12×10^{-10} meter (1 to 4 bohrs). A weighted average of the interaction energies of the three equilibrium configurations was then taken.

The interaction energies obtained were within the scatter of other ab initio calculations and had the proper qualitative behavior. However, they tended to be higher than other published values.

Neither the dipole moment nor its derivative with respect to H_2 internuclear distance

had been previously calculated. The values obtained by the valence-bond model appeared to have the correct trends at large intermolecular distances and to be consistent with values obtained classically with one minor exception: the sign of the small transverse component was different for the valence-bond and classical methods. This was attributed to a lack of polarizability of the H atom in the valence-bond model for large intermolecular distances.

The electric dipole moment and its derivative can be used to calculate pressure-induced vibrational absorption coefficients.

Lewis Research Center,
    National Aeronautics and Space Administration,
        Cleveland, Ohio, May 8, 1973,
            503-04.

APPENDIX - SYMBOLS

$(ab\bar{c})$ shorthand notation for antisymmetrized product of orthogonalized spin-orbitals

$\underline{C}$ column vector of coefficients of ψ_j

$\underline{C}'$ column vector of coefficients of φ_i

C_l expansion coefficient for μ_z

C_{pj} j^{th} Cartesian coordinate of proton p

$\bar{C}_{ppj}$ j^{th} Cartesian coordinate of center of atomic charge p

$\bar{C}_{pqj}$ j^{th} Cartesian coordinate of center of overlap charge pq

C'_r element of $\underline{C}'$

D_l expansion coefficient for $\partial\mu_z/\partial r$

$\underline{d}$ matrix of overlap eigenvalues

$\underline{d}^{-1/2}$ inverse square root of $\underline{d}$

$d_{ii}^{-1/2}$ diagonal element of $\underline{d}^{-1/2}$

E electronic and nuclear repulsion energy of complex

E_{at} energy of atom

E_e electronic energy

$E_{int,A}$ interaction energy for configuration A

$\bar{E}_{int}$ average interaction energy

E_m electronic and nuclear repulsion energy of diatomic molecule

$\bar{F}_{ij}$ one-electron integral of orthogonalized orbitals

f_i expansion coefficient for E_{int}

$\bar{G}_{ijkl}$ two-electron integral of orthogonalized orbitals

G_{lm} expansion coefficient for $2^{-1/2}(\mu_x + i\mu_y)$

G_{mnop} two-electron integral of 1s orbitals

$\underline{H}$	Hamiltonian matrix with basis functions ψ_j
$\hat{H}$	Hamiltonian operator for electrons
H_{nk}	element of $\underline{H}$
$\underline{H}_\varphi$	Hamiltonian matrix with basis functions φ_i
$\left(H_\varphi\right)_{ij}$	element of $\underline{H}_\varphi$
$\hbar$	Planck constant divided by 2π
i	$(-1)^{1/2}$
J_{lm}	expansion coefficient for $\partial/\partial r \left[2^{-1/2}(\mu_x + i\mu_y)\right]$
K_{kl}	kinetic energy integral
L_{jkp}	nuclear attraction integral
$\underline{M_\chi^{-1/2}}$	Löwdin transformation matrix
$\left(M_\chi^{-1/2}\right)_{ki}$	element of $\underline{M_\chi^{-1/2}}$
m	integer in expansions in normalized associated Legendre functions
$n_{rs}^{m\alpha n\alpha}$	coefficients of spin-orbital products with two α spins
$n_{rs}^{m\beta n\beta}$	coefficients of spin-orbital products with two β spins
P'_{mn}	electron population in the orbital density $\chi'_m \chi'_n$ irrespective of spin state
P_{pq}	electron population in the orbital density $\chi_p \chi_q$ irrespective of spin state
$\underline{\mathscr{P}}$	matrix of $\mathscr{P}_{pq}$
$\mathscr{P}_{pq}$	normalized one-electron population
Q	scalar quadrupole moment
Q'	$\partial Q/\partial r$
$\check{q}$	$(\zeta_p - \zeta_q)R_{pq}/2$ (subscripts vary)
R_{pq}	distance between points p and q
R_r	intermolecular distance (see fig. 1)
r	internuclear distance of diatomic molecule

30

r_{ij}	distance between electron or proton i and electron j
$\underline{S}$	matrix of S_{pq}
S_{pq}	overlap integral for χ_p and χ_q
$\underline{U}$	unitary matrix
$\underline{\tilde{U}}$	transpose of $\underline{U}$
$\underline{V}$	matrix relating $\underline{\psi}$ and $\underline{\varphi}$
$\underline{\tilde{V}}$	transpose of $\underline{V}$
v_i	volume in configuration space for electron i
W_i, W_{ij}	expansion coefficient for E_{int}
w_{pq}	$(\zeta_p + \zeta_q)R_{pq}/2$
x, y, z	Cartesian coordinates
α	polarizability
$\alpha(i)$	spin eigenfunction of electron i with component of spin angular momentum along the axis of quantization equal to $\hbar/2$
$\beta(i)$	spin eigenfunction of electron i with component of spin angular momentum along the axis of quantization equal to $-\hbar/2$
Δ_{pq}	displacement of overlap charge center from p-q geometric center, measured in direction from p towards q and expressed in units of R_{pq}
ζ	orbital exponent
ζ_p	orbital exponent of χ_p
ζ_{po}	approximate optimum orbital exponent of χ_p
Θ_i	normalized Legendre polynomial
Θ_{ij}	normalized associated Legendre function
θ	angle between internuclear axis of molecule and line through atom bisecting the molecule
μ_j	j^{th} component of electric dipole moment
τ	volume in configuration and spin space of three electrons
Φ	azimuthal angle about z axis

$\underline{\varphi}$ row vector with elements φ_i

φ_i antisymmetrized product of orthogonalized spin orbitals

$\underline{\chi}$ row vector with elements χ_p

$\underline{\chi}'$ row vector with elements χ'_p

$\chi_p(i)$ $1s$ orbital of electron i centered on proton p

$\chi'_p(i)$ orthogonalized orbital of electron i

Ψ wave function of system

$\underline{\psi}$ row vector with elements ψ_j

ψ_j formal orthogonalized valence-bond structure

Ω solid angle for molecule orientation

∇_i^2 Laplacian operator for the coordinates of electron i

32

REFERENCES

1. Patch, R. W.: Calculated Pressure-Induced Vibrational Absorption in H_2-H_2 Collisions in Hydrogen Gas. NASA TN D-6155, 1971.

2. Porter, R. N.; and Karplus, M.: Potential Energy Surface for H_3. J. Chem. Phys., vol. 40, no. 4, Feb. 15, 1964, pp. 1105-1115.

3. Hirschfelder, J.; Eyring, H.; and Rosen, N.: I. Calculation of Energy of H_3 Molecule. J. Chem. Phys., vol. 4, no. 2, Feb. 1936, pp. 121-130.

4. Hirschfelder, J.; Diamond, H.; and Eyring, H.: Calculation of the Energy of H_3 and of H_3^+. III. J. Chem. Phys., vol. 5, no. 9, Sept. 1937, pp. 695-703.

5. Stevenson, David; and Hirschfelder, Joseph: The Structure of H_3, H_3^+, and of H_3^-. IV. J. Chem. Phys., vol. 5, no. 12, Dec. 1937, pp. 933-940.

6. Hirschfelder, Joseph O.: The Energy of the Triatomic Hydrogen Molecule and Ion, V. J. Chem. Phys., vol. 6, no. 12, Dec. 1938, pp. 795-806.

7. Walsh, J. M.; and Matsen, F. A.: Molecular Orbital Calculations for H_3. J. Chem. Phys., vol. 19, no. 5, May 1951, pp. 526-528.

8. Barker, Roland S.; Eyring, Henry; Thorne, Charles J.; and Baker, Don A.: Use of Electron Repulsion Integral Approximations in Molecular Quantum Mechanics. J. Chem. Phys., vol. 22, no. 4, Apr. 1954, pp. 699-702.

9. Barker, Roland S.; and Eyring, Henry: Use of Nuclear Attraction Integral Approximations in Molecular Quantum Mechanics. J. Chem. Phys., vol. 22, no. 7, July 1954, pp. 1182-1188.

10. Boys, S. F.; Cook, G. B.; Reeves, C. M.; and Shavitt, I.: Automatic Fundamental Calculations of Molecular Structure. Nature, vol. 178, no. 48, Dec. 1, 1956, pp. 1207-1209.

11. Snow, Richard; and Eyring, Henry: Activated Complex Energies. J. Phys. Chem., vol. 61, no. 1, Jan. 30, 1957, pp. 1-6.

12. Ransil, Bernard J.: Application of Configuration Interaction to the H_3 Complex. J. Chem. Phys., vol. 26, no. 4, Apr. 1957, p. 971.

13. Kimball, George E.; and Trulio, John G.: Quantum Mechanics of the H_3 Complex. J. Chem. Phys., vol. 28, no. 3, Mar. 1958, pp. 493-497.

14. Meador, Willard E., Jr.: Calculation of the Energies of Triatomic Hydrogen Using a Modified Roothaan Procedure. J. Chem. Phys., vol. 29, no. 6, Dec. 1958, pp. 1339-1345.

15. Aroeste, Henry; and Jameson, William J., Jr.: Short-Range Interaction Between a Hydrogen Molecule and a Hydrogen Atom. J. Chem. Phys., vol. 30, no. 2, Feb. 1959, pp. 372-374.

16. Grigging, Virginia; Jackson, Julius L.; and Ransil, Bernard J.: Magnetic Interaction of H_3. J. Chem. Phys., vol. 30, no. 4, Apr. 1959, pp. 1066-1074.

17. Oleari, Luigi; Carra, Sergio; and Simonetta, Massimo: Geometria e Struttura Elettronica di Alcuni Complessi Attivati - Nota II. Sul Calcolo dell'energia di Attivazione per la Reazione $H + H_2$. Gazzetta Chim. Italianna, vol. 91, no. 12, Dec. 1961, pp. 1413-1419.

18. Bradley, J. N.: Quantum Mechanics of the H_3 Complex. Trans. Faraday Soc., vol. 60, no. 8, Aug. 1964, pp. 1353-1362.

19. Hoyland, James R.: Two-Center Wavefunctions for ABH_n Systems. Illustrative Calculations on H_3^+ and H_3. J. Chem. Phys., vol. 41, no. 5, Sept. 1, 1964, pp. 1370-1376.

20. Krauss, Morris: Calculation of the Geometrical Structure of Some AH_n Molecules. J. Res. Nat. Bur. Std., vol. 68A, no. 6, Nov.-Dec. 1964, pp. 635-644.

21. Edmiston, C.; and Krauss, M.: Configuration-Interaction Calculation of H_3 and H_2. J. Chem. Phys., vol. 42, no. 3, Feb. 1, 1965, pp. 1119-1120.

22. Conroy, Harold; and Bruner, Buddy L.: Energy Surface for the Linear H_3 System. J. Chem. Phys., vol. 42, no. 11, June 1, 1965, pp. 4047-4048.

23. Harris, F. E.; Micha, D. A.; and Pohl, H. A.: The Interaction Potential Surface for H_3. Arkiv. f. Fysik, vol. 30, no. 20, Oct. 1965, pp. 259-266.

24. Bowen, H. C.; and Linnett, J. W.: Quantum-Mechanical Study of the Transition State in the H_3 System. Trans. Faraday Soc., vol. 62, no. 11, Nov. 1966, pp. 2953-2954.

25. Considine, J. P.; and Hayes, E. F.: Single-Center Wavefunctions for H_3^+ and H_3. J. Chem. Phys., vol. 46, no. 3, Feb. 1, 1967, pp. 1119-1124.

26. Conroy, Harold; and Bruner, Buddy L.: Molecular Schrodinger Equation. VI. Results for H_3 and Other Simple Systems. J. Chem. Phys., vol. 47, no. 3, Aug. 1, 1967, pp. 921-930.

27. Shavitt, I.; Stevens, R. M.; Minn, F. L.; and Karplus, M.: Potential-Energy Surface for H_3. J. Chem. Phys., vol. 48, no. 6, Mar. 15, 1968, pp. 2700-2713.

28. Schwartz, Maurice E.; and Schaad, L. J.: Ab Initio Studies of Small Molecules Using 1s Gaussian Basis Functions. III. LCGTO SCF MO Wavefunctions of the Three- and Four-Electron Systems He_2^+, He_2, and Linear H_3, H_4^+, H_4. J. Chem. Phys., vol. 48, no. 10, May 15, 1968, pp. 4709-4715.

29. Edmiston, C.; and Krauss, M.: Pseudonatural Orbitals as a Basis for the Superposition of Configurations. II. Energy Surface for Linear H_3. J. Chem. Phys., vol. 49, no. 1, July 1, 1968, pp. 192-205.

30. Porter, R. N.; Stevens, R. M.; and Karplus, M.: Symmetric H_3: A Semiempirical and Ab Initio Study of a Simple Jahn-Teller System. J. Chem. Phys., vol. 49, no. 11, Dec. 1, 1968, pp. 5163-5178.

31. Trivedi, P. C.: The Short-Range Interaction Between a Hydrogen Molecule and a Hydrogen Atom. Physica, vol. 48, no. 4, Sept. 30, 1970, pp. 486-496.

32. Margenau, Henry: The Forces Between a Hydrogen Molecule and a Hydrogen Atom. Phys. Rev., vol. 66, no. 11-12, Dec. 1 and 15, 1944, pp. 303-306.

33. Mason, Edward A.; and Hirschfelder, Joseph O.: Short-Range Intermolecular Forces. II. H_2-H_2 and H_2-H. J. Chem. Phys., vol. 26, no. 4, Apr. 1957, pp. 756-766.

34. Amdur, I.: Repulsive Interaction Potentials at Small Interaction Distances: He-He and H-H_2 Systems. J. Chem. Phys., vol. 17, no. 9, Sept. 1949, pp. 844-845.

35. Schulz, W. R.; and LeRoy, D. J.: Kinetics of the Reaction H+p-H_2=o-H_2+H. J. Chem. Phys., vol. 42, no. 11, June 1, 1965, pp. 3869-3873.

36. Karplus, M.; and Porter, R. N.: General Discussion on Molecular Dynamics of the Chemical Reactions of Gases. Disc. Faraday Soc., no. 44, 1967, pp. 164-166.

37. Geddes, J.; Krause, H. F.; and Fite, W. L.: Results on the Reaction D+$H_2 \rightarrow$ HD+H Using Modulated Crossed Beams. J. Chem. Phys., vol. 52, no. 6, Mar. 15, 1970, pp. 3296-3297.

38. Brumer, P.; and Karplus, M.: Differential Cross Sections for D+H_2: A Comparison with Experiment. J. Chem. Phys., vol. 54, no. 11, June 1, 1971, pp. 4955-4957.

39. McWeeny, R.: The Valence Bond Theory of Molecular Structure. I. Orbital Theories and the Valence-Bond Method. Proc. Roy. Soc. (London), Ser. A, vol. 223, no. 1152, Apr. 7, 1954, pp. 63-79.

40. McWeeny, R.: The Valence-Bond Theory of Molecular Structure. II. Reformulation of the Theory. Proc. Roy. Soc. (London), Ser. A, vol. 223, no. 1154, May 6, 1954, pp. 306-323.

41. Magnasco, V.; and Musso, G. F.: Quantum Mechanics of the H_2-H_2 Interaction. I. A Restricted Valence-Bond Approach. J. Chem. Phys., vol. 46, no. 10, May 15, 1967, pp. 4015-4025.

42. Magnasco, V.; and Musso, G. F.: Quantum Mechanics of the H_2-H_2 Interaction. II. A Full Valence-Bond Calculation. J. Chem. Phys., vol. 47, no. 5, Sept. 1, 1967, pp. 1723-1730.

43. Patch, R. W.: Calculated Interaction Energy and Dipole Moment in Collisions of Two Hydrogen Molecules. NASA TN D-5486, 1969.

44. Weinbaum, Sidney: The Normal State of the Hydrogen Molecule. J. Chem. Phys., vol. 1, no. 8, Aug. 1933, pp. 593-596.

45. Spindler, R. J., Jr.: Franck-Condon Factors for Band Systems of Molecular Hydrogen. - I. The $(B^1\Sigma_u^+ - X^1\Sigma_g^+)$, $(I^1\Pi_g - B^1\Sigma_u^+)$, and $(d^3\Pi_u - a^3\Sigma_g^+)$ Systems. J. Quant. Spectrosc. Radiat. Transfer, vol. 9, no. 5, May 1969, pp. 597-626.

46. Löwdin, Per-Olov: Quantum Theory of Cohesive Properties of Solids. Adv. Phys., vol. 5, no. 17, Jan. 1956, pp. 3-172.

47. Slater, John C.: Quantum Theory of Molecules and Solids. Vol. I. Electronic Structure of Molecules. McGraw-Hill Book Co., Inc., 1963, p. 50.

48. Magnasco, Valerio; and Musso, Gianfranco: Population Analysis of Many Configuration Wave Functions. Atti dell Accademia Ligure di Scienze e Lettere, vol. 22, 1965, pp. 383-389.

49. Pauling, Linus: The Calculation of Matrix Elements for Lewis Electronic Structures of Molecules. J. Chem. Phys., vol. 1, no. 4, Apr. 1933, pp. 280-283.

50. Slater, J. C.: Molecular Energy Levels and Valence Bonds. Phys. Rev., vol. 38, no. 6, Sept. 15, 1931, pp. 1109-1144.

51. Slater, John C.: Quantum Theory of Atomic Structure. Vol. I. McGraw-Hill Book Co., Inc., 1960, pp. 113-119.

52. Pauling, Linus; and Wilson, E. Bright, Jr.: Introduction to Quantum Mechanics with Applications to Chemistry. McGraw-Hill Book Co., Inc., 1935, p. 185.

53. Kolos, W.; and Wolniewicz, L.: Potential-Energy Curves for the $X^1\Sigma_g^+$, $b^3\Sigma_u^+$, and $C^1\Pi_u$ States of the Hydrogen Molecule. J. Chem. Phys., vol. 43, no. 7, Oct. 1, 1965, pp. 2429-2441.

"The aeronautical and space activities of the United States shall be conducted so as to contribute . . . to the expansion of human knowledge of phenomena in the atmosphere and space. The Administration shall provide for the widest practicable and appropriate dissemination of information concerning its activities and the results thereof."

—NATIONAL AERONAUTICS AND SPACE ACT OF 1958

NASA SCIENTIFIC AND TECHNICAL PUBLICATIONS

TECHNICAL REPORTS: Scientific and technical information considered important, complete, and a lasting contribution to existing knowledge.

TECHNICAL NOTES: Information less broad in scope but nevertheless of importance as a contribution to existing knowledge.

TECHNICAL MEMORANDUMS: Information receiving limited distribution because of preliminary data, security classification, or other reasons. Also includes conference proceedings with either limited or unlimited distribution.

CONTRACTOR REPORTS: Scientific and technical information generated under a NASA contract or grant and considered an important contribution to existing knowledge.

TECHNICAL TRANSLATIONS: Information published in a foreign language considered to merit NASA distribution in English.

SPECIAL PUBLICATIONS: Information derived from or of value to NASA activities. Publications include final reports of major projects, monographs, data compilations, handbooks, sourcebooks, and special bibliographies.

TECHNOLOGY UTILIZATION PUBLICATIONS: Information on technology used by NASA that may be of particular interest in commercial and other non-aerospace applications. Publications include Tech Briefs, Technology Utilization Reports and Technology Surveys.

Details on the availability of these publications may be obtained from:

SCIENTIFIC AND TECHNICAL INFORMATION OFFICE

NATIONAL AERONAUTICS AND SPACE ADMINISTRATION

Washington, D.C. 20546